Chapter 4. Energy-Based Excess Pore Pressure Generation Models

4.1 Introduction

Corollary to liquefaction evaluation procedures are excess pore pressure generation models. This can be understood because liquefaction, as defined in this thesis, is the condition where the excess pore pressure (u_{xs}) is equal to the initial effective overburden (σ'_{vo}). Therefore, if parameters such as stress, strain, and energy can be related to one value of u_{xs} (i.e., $u_{xs} = \sigma'_{vo}$), it should be expected that the same parameters can also be related to other values of u_{xs}, and in fact, they have. Both stress- and strain-based pore pressure models have been developed and are commonly used in numerical modeling of soils subjected to cyclic loading (e.g., Booker et al. 1976 and Martin et al. 1975).

In addition to stress- and strain-based models, numerous energy-based excess pore pressure generation models have been developed. Nemat-Nasser and Shokooh (1979) established governing differential equations relating energy dissipation to the densification of dry samples and to the generation of excess pore pressures in saturated samples. Complementing Nemat-Nasser and Shokooh's theoretical work are numerous empirical relations (e.g., Simcock et al. 1983, Law et al. 1990, Green et al. 2000). Although these pore pressure models provide credence to quantifying soil *Capacity* in terms of dissipated energy, the dependence of the models' calibration parameters on factors other than the soil's density, fabric, and stress state (i.e., state variables) needs to be examined. Because earthquake motions have very different amplitudes, frequency content, and durations in comparison to the motions imparted to the soil by various remediation techniques, the dependence of calibration parameters on the nature of the loading, as well as state variables, may inherently limit the usefulness of *Capacity* curves developed from earthquake case histories for remedial ground densification design.

Several energy-based pore pressure generation models from literature are reviewed in this chapter. Additionally, from the analysis of numerous cyclic triaxial test data, a new expression is presented relating dissipated energy and pore pressure generation. The proposed model is referred to as the *GMP* Model to denote the authors of the publication

in which it was first proposed: *G*reen, *M*itchell, and *P*olitio (Green et al. 2000). The *GMP* Model is similar in form to several of earlier proposed models, but only has one calibration parameter (*PEC*: pseudo energy capacity). Established correlations for *PEC* are presented and discussed, with particular emphasis on the variation of *PEC* with respect to the amplitude of the applied loading.

4.2 Energy-Based Pore Pressure Models from Published Literature

A thorough literature review was performed and selected energy-based pore pressure models are presented below. The large number of the models necessitates a "cookbook" presentation style similar to that used in Chapter 2 in presenting the energy-based liquefaction evaluation procedures. With the exceptions of the models proposed by Nemat-Nasser and Shokooh (1979) and Mostaghel and Habibaghi (1979), all of the expressions relating excess pore pressure generation and dissipated energy are empirical curve fit equations of laboratory data. The models relate the dissipated energy per unit volume of material (ΔW) to the residual excess pore pressures (u_{xs}), where u_{xs} is defined as the pore pressure in excess of hydrostatic conditions when the applied cyclic stress is zero. Where possible, the models are presented in terms of pore pressure ratio (r_u), which is defined as u_{xs} divided by the initial effective overburden stress (σ'_{vo}).

For each of the proposed models, an expression relating r_u and ΔW is given, followed by the values of the calibration parameters and information on the laboratory tests on which the models are based. For many of the models, procedures for determining the calibration parameters from laboratory data were not given in the referenced literature. Also, many of the details about the laboratory test data are incomplete. The validity of the models may be limited to the specific test conditions (e.g., load path and amplitude, effective confining stress) and soil types on which they are based. To provide a consistent presentation of the models, several of the expressions are presented in alternate forms from those in the referenced literature. However, the underlying assumptions on which the models are based are unchanged. Comparison of the models is not possible because few of the have correlations relating calibration parameters to soil properties

(e.g., D_r or $N_{1,60}$). However, Section 4.3 provides limited commentaries on several of the proposed models.

4.2.1 *N-NS* Model (Nemat-Nasser and Shokooh 1977, 1979)

Model:

$$r_u = \left[1 - \frac{\Delta W \left(e_o - e_{\min} \right)^b}{\hat{u}\, e_o} \right]^{\frac{1}{1-a}} - 1 \qquad (4\text{-}1)$$

where: ΔW = Dissipated energy per unit volume of material (*psi*).

e_o = Initial void ratio of the soil.

$e_{\min}$ = Minimum void ratio of the soil.

a, b = Calibration parameters.

$\hat{u} = \dfrac{v'}{(a-1)\cdot \eta_w}$

η_w = Bulk modulus of water (*psi*).

v' = Calibration parameter.

Calibration Parameters: $a = 2.5$

$b = 3.5$

$\dfrac{h}{\hat{u}} = 7.41 \times 10^5$

From laboratory tests, the following relation may be used to determine h:

$\Delta W = h \cdot N \cdot CSR^{1+\alpha}$

α = 2.5

h = Calibration parameter, specific value not given.

CSR = Cyclic stress Ratio.

N = Number of cycles of loading.

Soil and Effective Confining stress: Ref. Lab data: DeAlba et al. (1976)

Monterey No. 0 ($e_{min} = 0.564$, $e_{max} = 0.852$)

$\sigma'_{vo} = 30$ to $55 kPa$

D_r = 54 and 68%

Test Apparatus and Loading:

Large scale simple shear tests

Stress-controlled

CSR = 0.104 to 0.185

4.2.2 *MH* Model (Mostaghel and Habibaghi 1978, 1979)

Model:

$$r_u = \frac{1}{e_o}\frac{\Delta W}{\sigma'_{vo}} \tag{4-2}$$

where: ΔW = Dissipated energy per unit volume of material.

e_o = Initial void ratio of the soil.

σ'_{vo} = Initial vertical effective stress.

ΔW and σ'_{vo} have the same units. Mostaghel and Habibaghi (1978, 1979) did not propose Equation (4-2) as a formal pore pressure generation model, but they assumed this relation in deriving their liquefaction evaluation procedure.

4.2.3 *DB1* Model (Davis and Berrill 1982)

Model:

$$r_u = \alpha\frac{\Delta W}{\sigma'_{vo}} \tag{4-3}$$

where: ΔW = Dissipated energy per unit volume of material.

σ'_{vo} = Initial vertical effective stress.

α = Calibration parameter.

ΔW and σ'_{vo} have the same units, and α is dimensionless.

Calibration Parameter: $50 \le \alpha \le 80$ (Davis and Berrill 2001)

Soil and Effective Confining stress: Ref. lab data: Simcock et al. (1983)

New Brighton Sand

Moist tamped

Isotropically consolidated

σ'_o =50, 100, 150*kPa*

D_r = 67 to 95%

Test Apparatus and Loading:

Cyclic triaxial

Stress-controlled

CSR = 0.127 to 0.293

4.2.4 *BD* Model (Berrill and Davis 1985)

Model:

$$r_u = \alpha' \left(\frac{\Delta W}{\sigma'_{vo}} \right)^{\beta} \tag{4-4}$$

where: ΔW = Dissipated energy per unit volume of material.

σ'_{vo} = Initial vertical effective stress.

α', β = Calibration parameters.

ΔW and σ'_{vo} have the same units, and α' and β are dimensionless.

Calibration Parameter: (α', β): (0.8, 0.6), (0.65, 0.5), and (0.5, 0.5)

"... β = 0.5 appears to be optimal."

Soil and Effective Confining stress, Test Apparatus and Loading:

Same as for *DB1* Model

4.2.5 *DB2* Model (Davis and Berrill 2001)

Model:

$$r_u = 1 - \exp(-\alpha \frac{\Delta W}{\sigma'_{vo}}) \tag{4-5}$$

where: ΔW = Dissipated energy per unit volume of material.

σ'_{vo} = Initial vertical effective stress.

α = Calibration parameter.

ΔW and σ'_{vo} have the same units, and α is dimensionless.

Calibration Parameter: $50 \le \alpha \le 80$

Soil and Effective Confining stress, Test Apparatus and Loading:

Same as for *DB1* Model

4.2.6 *YTI* Model (Yamazaki, Towhata, and Ishihara 1985)

Model:

$$r_u = \begin{cases} \dfrac{1}{1+\left(\dfrac{b\sigma'_{vo}}{\Delta W}\right)^a} & for \quad r_u \le 0.5 \\ \dfrac{a}{4}\cdot\left[\ln\left(\dfrac{\Delta W}{\sigma'_{vo}}\right)-\ln(b)\right]+0.5 & for \quad 0.5 < r_u \le 1.0 \end{cases} \tag{4-6}$$

where: ΔW = Dissipated energy per unit volume of material.

σ'_{vo} = Initial vertical effective stress.

a,b = Calibration parameters.

ΔW and σ'_{vo} have the same units, and a and b are dimensionless.

Calibration Parameters: $a = 0.848$, $b = 2.04 \times 10^{-3}$ } Toyoura Sand: $\sigma'_o = 294kPa$, $D_r = 40$ to 50%

The calibration parameters can be determined from laboratory test data as shown in Figure 4-1.

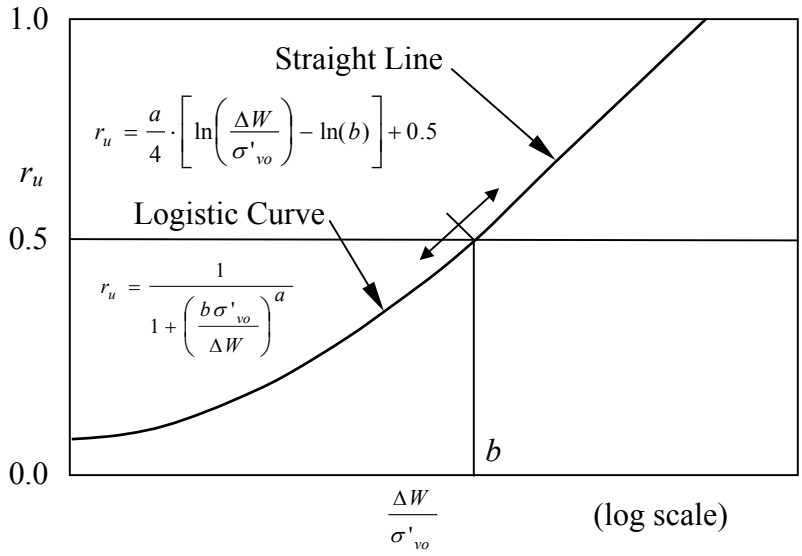

Figure 4-1. Procedure for determining calibration parameters for *YTI* Model from laboratory test data. (Adapted from Yamazaki et al. 1985).

Soil and Effective Confining stress: Ref: Lab data Towhata and Ishihara (1985)

Toyoura Sand

Air pluviated samples

Isotropically consolidated

$\sigma'_o = 294kPa$

$D_r = 42$ to 51% (torsional shear)

$D_r = 42$ to 49% (triaxial)

Test Apparatus and Loading:

Hollow cylinder triaxial-torsional shear

Stress-controlled loading

Various load paths including torsional shear and triaxial

CSR = 0.188 to 0.264 (torsional shear)

CSR = 0.184 to 0.194 (triaxial)

Load rate=0.14*% strain/min*

4.2.7 *LCH* Model (Law, Cao, and He 1990)

Model:

$$\frac{u_{xs}}{\sigma'_{ho}} = \alpha W_N^{\beta} \tag{4-7}$$

where: W_N = Dissipated energy parameter.

$$= F_1(K_c) F_2(D_r) \frac{\Delta W}{\sigma'_{ho}}$$

ΔW = Dissipated energy per unit volume of material.

$F_1(K_c)$ = Normalizing function to account for K_c.

$$= 1 - \xi \log(K_c)$$

$F_2(D_r)$ = Normalizing function to account for D_r.

$$= 10^{\varsigma(D_r - 0.70)}$$

$K_c = \sigma'_{vo}/\sigma'_{ho}$

Dr = Relative Density.

σ'_{ho} = Initial horizontal effective stress.

σ'_{vo} = Initial vertical effective stress.

$\alpha, \beta, \xi, \zeta$ = Calibration parameters.

u_{xs} = Excess pore pressure.

ΔW, u_{xs}, σ'_{vo}, and σ'_{ho} have the same units, and α, β, ξ, and ζ are dimensionless.

Calibration Parameters: $\xi = 3.0$

$\zeta = -2.0$

No values are given for α and β

Soil and Effective Confining stress:

Fujian Standard sand

Moist tamped

Isotropically consolidated

σ'_o =50, 100, 150*kPa*

$D_r = 70\%$

Anisotropic consolidated

$\sigma'_{ho} = 100kPa$

K_c = 1.5, 1.75, and 2.0

$D_r = 70\%$

Test Apparatus and Loading:

Cyclic triaxial and Hollow cylinder torsional shear

Stress-controlled

Load rate: 1.0*hz*

4.2.8 *YS* Model (Yanagisawa and Sugano 1994)

Model:

$$r_u = \frac{S'_s}{a + bS'_s} \tag{4-8}$$

where: S'_s = State parameter.

$$= \frac{dW}{\sigma'_m}$$

dW = Increment in dissipated energy per unit volume of material.

σ'_m = Mean effective stress.

a,b = Calibration parameters.

dW and σ'_m have the same units, and a and b are dimensionless. It is unclear whether the σ'_m is the initial mean confining stress or the mean confining stress at the time of the increment dW.

Calibration Parameters: No values for a and b are given.

Soil and Effective Confining stress and Test Apparatus and Loading:

Strain-controlled cyclic triaxial

Toyoura sand

Air pluviated

Isotropically consolidated

σ'_o = 196, 294, 343*kPa*

D_r = 40, 70%

γ_{cyc} = 0.24, 0.38, 0.47, 0.50, 0.56, 0.60%, and random

Load rate: 0.5*hz*

Strain-controlled torsional shear

Samples prepared by *MSP* Method (Miura and Toki 1982)

Isotropically consolidated

σ'_o = 196*kPa*

D_r = 49, 81%

γ_{cyc} = 0.2, 0.5, 1.0%

Two-Directional Cubic Shear

K_o consolidated

σ'_{vo} = 49*kPa*

D_r = 61%

4.2.9 *Hsu* Model (Hsu 1995)

Model:

$$r_u = a\left(\frac{\Delta W}{\sigma'_{vo}}\right)^b \tag{4-9}$$

where: ΔW = Dissipated energy per unit volume of material.

σ'_{vo} = Initial vertical effective stress.

a, b = Calibration parameters.

ΔW and σ'_{vo} have the same units, and a and b are dimensionless.

Calibration Parameters: $a = (400 - 420\,D_r)CSR^2$

$b = (1.9 - 1.25\,D_r)CSR^{1/2}$

CSR = Cyclic stress ratio.

D_r = Relative Density.

Soil and Effective Confining stress:

Chu-An sand

Air pluviated

Isotropically consolidated

σ'_o = 50, 100, 200*kPa*

D_r = 35, 50, 80*%*

Test Apparatus and Loading:

Hollow cylinder apparatus

Stress-controlled torsional shear

CSR = 0.16, 0.19, and 0.22

Load rate: 1.0*hz*

4.2.10 *Liang* Model (Liang 1995)

Model:

$$r_u = a + \frac{b\,\Delta W}{c + \Delta W} \tag{4-10}$$

where: ΔW = Dissipated energy per unit volume of material.

σ'_{vo} = Initial vertical effective stress.

a,b,c = Calibration parameters.

ΔW and σ'_{vo} have the same units, and *a*, *b*, and *c* are dimensionless.

Calibration Parameters:

	Dr (%)	*a*	*b*	*c*
Reid	54.9	0.03663	1.30619	0.36743
Bedford	58.3	0.00233	1.36265	0.47798
sand	67.5	0.00663	1.14189	0.35988
LSFD	60.0	0.05891	1.2216	0.228
silty-	71.2	0.00336	1.2847	0.208
sand	87.4	0.03	1.66	0.159

Soil and Effective Confining stress:

Reid Bedford sand and

Lower San Fernando Dam silty-sand (*FC* < 28*%*)

Dry tapped

Isotropically consolidated

$\sigma'_o = 82.7kPa$

$D_r = 54.9, 58.3, 67.5\%$ (Reid Bedford)

$D_r = 59.9, 71.2, 87.4\%$ (*LSFD*)

Test Apparatus and Loading:

Hollow cylinder torsional shear

Stress-controlled

Random earthquake type loading

4.2.11 *OAY* Model (Ogawa, Abe, and Yoshitsugu 1995)

Model:

$$u_{xs} \propto \Delta W^{0.5} \tag{4-11}$$

where: ΔW = Dissipated energy per unit volume of material.

u_{xs} = Pore pressure ratio.

ΔW and u_{xs} have the same units.

Calibration Parameters: None

Soil and Effective Confining stress:

Toyoura sand

Isotropically consolidated

$\sigma'_o = 98kPa$

$D_r = 60\%$

Test Apparatus and Loading:

Hollow cylinder torsional shear

Stress-controlled

$CSR = 0.2$

Load rate: $0.1hz$

4.2.12 *FSKL* Model (Figueroa, Saada, Kern, and Liang 1997)

Model:

$$r_u = -A\Delta W\left(A\Delta W - 2\right) \tag{4-12}$$

where: ΔW = Dissipated energy per unit volume of material (*kPa*).

A = Calibration parameter.

The above model was derived from an empirical expression presented in Figueroa et al. (1997) relating shear modulus degradation to ΔW. In deriving this expression, it was assumed $G = G_{max}(1\text{-}r_u)^{0.5}$.

Calibration Parameters: $A = 151.52 - 1.10\,D_r - 27.89\,\gamma - 0.016\,\sigma'_o$ (Kern 1996)

$A = 165.6 - 1.44\,D_r - 9.09\,\gamma$ (Figueroa et al. 1997)

D_r = Relative Density (%).

γ = Shear strain (%).

σ'_o = Initial effective confining stress (*kPa*).

Soil and Effective Confining stress:

Reid Bedford sand

Dry tapped

Isotropically consolidated

σ'_o = 41.4, 82.7, 124.1*kPa*

D_r = 50, 60, 70%

Test Apparatus and Loading:

Hollow cylinder torsional shear

Strain-controlled

γ = 0.15, 0.47, and 1.02%

Load rate: 0.1*hz*

4.2.13 *WTK* Model (Wang, Takemura, and Kuwano 1997)

Model:

$$r_u = \frac{a\dfrac{\Delta W}{(\sigma'_{mo})^n}}{1 + b\dfrac{\Delta W}{(\sigma'_{mo})^n}} \qquad (4\text{-}13)$$

where: ΔW = Dissipated energy per unit volume of material.

σ'_{mo} = Initial mean effective confining stress (kPa).

a,b,n = Calibration parameters.

ΔW and σ'_{mo} have the same units, and a, b, and n are dimensionless.

Calibration Parameters:

I_p	2	5	10	30
FC(%)	8	12	16	37
a	70.4	65.9	12.5	3.39
b	65.9	62.9	13.7	4.87

I_p = Plasticity index.

FC = Fines content.

n = Calibration parameter (0.6 to 0.8).

Soil and Effective Confining stress:

Toyoura sand and Kawasaki clay mixtures

I_p = 2, 5, 10, and 30

Consolidated from slurry

Istropically consolidated

σ'_o = 98, 196, 392kPa

Test Apparatus and Loading:

Cyclic triaxial

Stress-controlled

CSR: 0.006 to 0.154 (I_p = 2)

0.0009 to 0.171 (I_p = 5)

0.023 to 0.231 (I_p = 10)

0.029 to 0.251 (I_p = 30)

Load rate: 0.01, 0.1, 0.2, and 1.0*hz* Kuwano (2000)

4.3 Commentaries on the Models

Although a detailed parameter study comparing the various pore pressure models cannot be performed due to the lack of correlations between the models' calibration parameters and state variables, limited commentaries are given for several of the models.

MH Model:

Rearrangement of the *MH* Model yields: $\Delta W = r_u e_o \sigma'_{vo}$. From this expression, it can be seen that the *MH* Model predicts that it will require more energy to liquefy loose soil (i.e., large e_o) than dense soil (i.e., small e_o). This is contrary to observed behavior of soil.

DB1 Model:

The *DB1* Model tends to over predict increases in pore pressures as the cumulative dissipated energy increases.

BD Model:

Berrill and Davis (1985) give three sets of values for the calibration parameters (α', β): (0.8, 0.6), (0.65, 0.5), and (0.5, 0.5). Figure 2 in Berrill and Davis (1985) shows that these values cover the range of their laboratory data. However, the author was unable to duplicate Berrill and Davis' Figure 2 using the published values for the calibration parameters in conjunction with the *BD* Model. It is uncertain whether this is due to an error in the published values of the calibration parameters or in the author's implementation of the model.

YTI Model:

Towhata and Ishihara (1985) present the results of an extensive laboratory study showing a unique relationship between dissipated energy and pore pressure generation. In every

figure in this paper, a smooth curve is fit to the data without mention of how the curve was generated. Due to the commonality of the authors, subject matter, and dates of publishing, it is assumed that this curve is the *YTI* Model, the mathematical treatise of which is presented in Yamazaki, Towhata, and Ishihara (1985).

LCH Model:

As opposed to using the standard definition for pore pressure ratio (i.e., $r_u = u_{xs}/\sigma'_{vo}$), Law et al. (1990) used u_{xs}/σ'_{ho}, without explanation. The most probable reason for this is that for anisotropically consolidated cyclic triaxial tests when $K_c > 1$, failure occurs in the sample when $u_{xs}/\sigma'_{ho} = 1$, while $u_{xs}/\sigma'_{vo} < 1$. This is due to the lack of lateral restraint on the sample and is the reason why anisotropically consolidated cyclic triaxial tests are not used to model *in-situ* conditions for level ground. Rather these tests represent conditions of initial static shear stress and are used to develop the K_α used in the stress-based liquefaction evaluation procedure (Chapter 2, Section 2.2.1). As shown in Seed and Harder (1990), the influence of initial static shear stress on soil *Capacity* is a function of both the amplitude of the static shear stress and the soil's relative density (D_r). However, the $F_1(K_c)$ normalizing function proposed by Law et al. (1990) is independent of D_r.

4.4 *GMP* Model (Green, Mitchell, and Polito 2000)

From analyzing numerous cyclic triaxial test data, the following empirical expression, denoted as the *GMP* Model, provides a simple and accurate relationship between residual excess pore pressure generation and the energy dissipated per unit volume of soil:

$$r_u = \sqrt{\frac{\Delta W}{PEC}} \tag{4-14}$$

where r_u and ΔW were defined previously and *PEC* (i.e., pseudo energy capacity) is a calibration parameter. By setting the calibration parameters α'and β in the *BD* Model (Section 4.2.4) equal to $1/PEC^{0.5}$ and 0.5, respectively, it can be seen that the *GMP* Model is actually a special case of the more general *BD* Model. Other models having similar forms include the *LCH*, *Hsu*, and *OAY* Models.

PEC can be determined from cyclic test data by plotting r_u versus the square root of ΔW. The square root of *PEC* is the value on the horizontal axis corresponding to the intersection of a straight line drawn through the origin and the point of $r_u = 0.65$ and a horizontal line drawn at $r_u = 1.0$. This process of determining *PEC* is illustrated graphically in Figure 4-2.

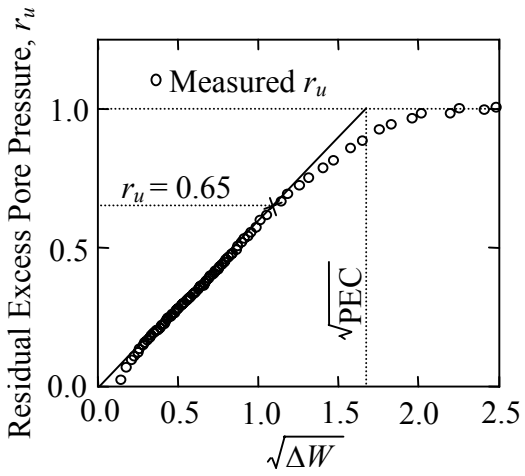

Figure 4-2. Graphic illustration of how *PEC* is determined from cyclic test data. The data shown in this figure is from a cyclic triaxial test conducted on Yatesville clean sand.

PEC can also be determined numerically using Equation (4-15).

$$PEC = \frac{\Delta W_{r_u=0.65}}{0.4225} \tag{4-15}$$

where $\Delta W_{ru=0.65}$ is the value of ΔW corresponding to $r_u = 0.65$. The term "pseudo energy capacity" or *PEC* is used to label the calibration parameter because it is approximately equal to ΔW at the point of initial liquefaction of the sample.

Comparisons of measured and predicted pore pressures for various samples subjected to cyclic triaxial and cyclic torsional loading, both stress and strain controlled, are shown in Figures 4-3a and 4-3b. As can be seen in these figures, the computed values of r_u closely match the measured values for a variety of soils and test conditions. These comparisons

are representative of those for several hundred cyclic tests, mainly stress-controlled cyclic triaxial tests.

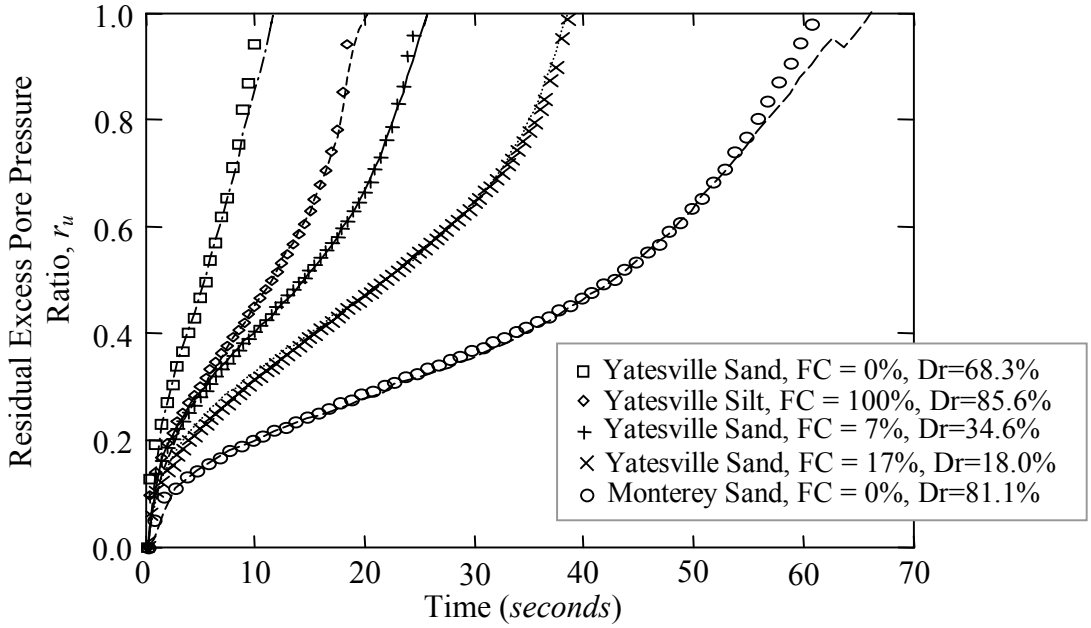

Figure 4-3a. Comparison of measured and computed residual excess pore pressures in various silt-sand mixtures having varying densities. Symbols are values computed using the *GMP* Model and the lines are the measured values. All samples were run in stress controlled cyclic triaxial tests. (Cyclic triaxial data is from Polito 1999).

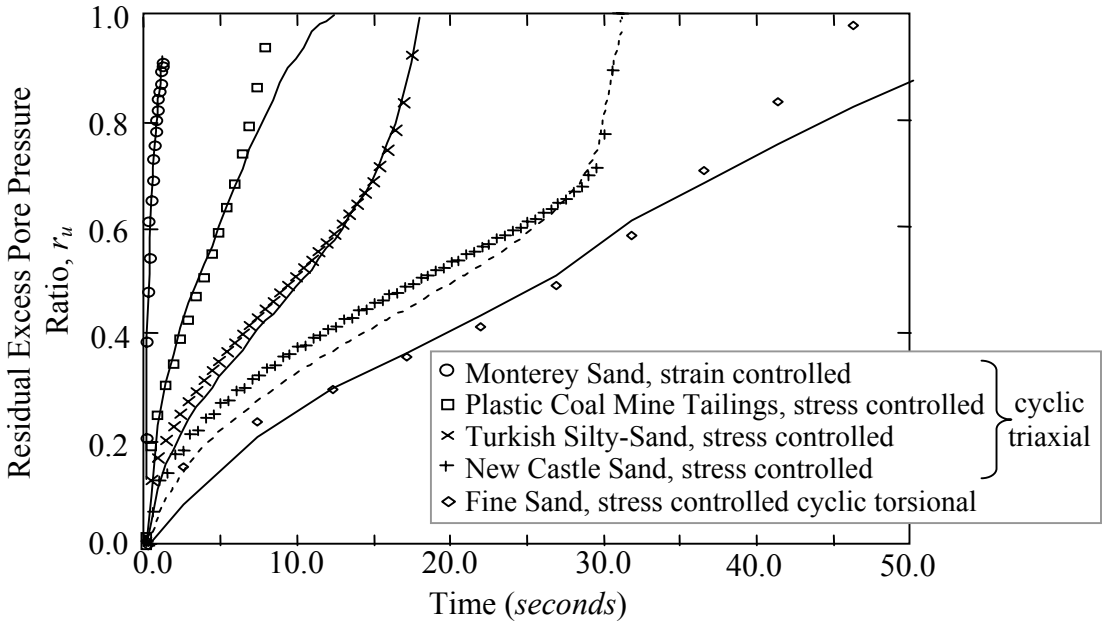

Figure 4-3b. Comparison of measured and computed residual excess pore pressures in samples tested in various configurations. Symbols are values computed using the *GMP* Model and the lines are the measured values. (Cyclic data is from Bonita 2000, Koester 1992, and Polito 1999).

From stress-controlled cyclic triaxial test data, correlations were developed relating *CSR*, *PEC*, and D_r for Monterey and Yatesville sands (i.e., medium and fine grained sands, respectively). All the samples were moist tamped, isotropically consolidated, and subjected to either 0.5*hz* or 1*hz* sinusoidal loading. The computed *PEC* values are listed in Table 5-2 in Chapter 5. Additional details about the laboratory tests can be found in Polito (1999). Equation (4-16) and (4-17) define the best-fit surfaces for the Monterey silt-sand and Yatesville silt-sand data, respectively. Based upon test results for specimens with non-plastic silt contents up to approximately 30%, the presence of the silt appears to have little or no influence on the computed *PEC*. This is in line with the findings of Polito (1999) who hypothesizes that the apparent increase in the *Capacity* of high fines content sand is actually attributed to the decrease in the penetration resistance of the silty sands. Given that relative density, and not penetration resistance, was used in the *PEC* correlations, silt content does not influence the correlation.

Monterey sand:

$$PEC = \begin{cases} -3.5 \cdot D_r \cdot CSR + 310.7 \cdot CSR^2 - 129.7 \cdot CSR \\ \quad + 14.3 + 0.7144 \cdot D_r + 0.01132 \cdot D_r^2 \\ \qquad\qquad for\ CSR \le 5.632 \times 10^{-3} \cdot D_r + 0.2087 \\ 1.463 \cdot 10^{-3} \cdot D_r^2 - 0.01613 \cdot D_r + 0.7644 \\ \qquad\qquad for\ CSR > 5.632 \times 10^{-3} \cdot D_r + 0.2087 \end{cases} \tag{4-16}$$

Yatesville sand:

$$PEC = \begin{cases} -1.64 \cdot D_r \cdot CSR + 310.7 \cdot CSR^2 - 110.2 \cdot CSR \\ \quad + 10.3 + 0.305 \cdot D_r + 0.0023 \cdot D_r^2 \\ \qquad\qquad for\ CSR \le 2.639 \times 10^{-3} \cdot D_r + 0.1773 \\ 1.359 \cdot 10^{-4} \cdot D_r^2 + 0.01416 \cdot D_r + 0.5285 \\ \qquad\qquad for\ CSR > 2.639 \times 10^{-3} \cdot D_r + 0.1773 \end{cases} \tag{4-17}$$

where *PEC* is in *kPa*, *CSR* is the cyclic stress ratio of the applied loading, and D_r is in percent.

Plots of Equations (4-16) and (4-17) are shown as contours of constant D_r in Figures 4-4 and 4-5, respectively, superimposed on laboratory data. Curve fitting in three dimensions (i.e., two independent variables and one independent variable) is as much an art as it is a mathematical process. In selecting the surfaces to fit the data, represented by Equations (4-16) and (4-17), an attempt was made to keep the geometry of the surfaces as simple as possible. In this vein, the same general shape was used for both the Yatesville and Monterey data. By doing this, the trends from one soil type were used to extrapolate the surface to regions of sparse data for the other soil type. As may be observed from these figures, there is a great deal of scatter in the data, implying that the two independent variables used in the correlation (i.e., D_r and *CSR*) do not completely account for the observed variation of *PEC*. Additional studies are required to refine the correlations shown in these figures.

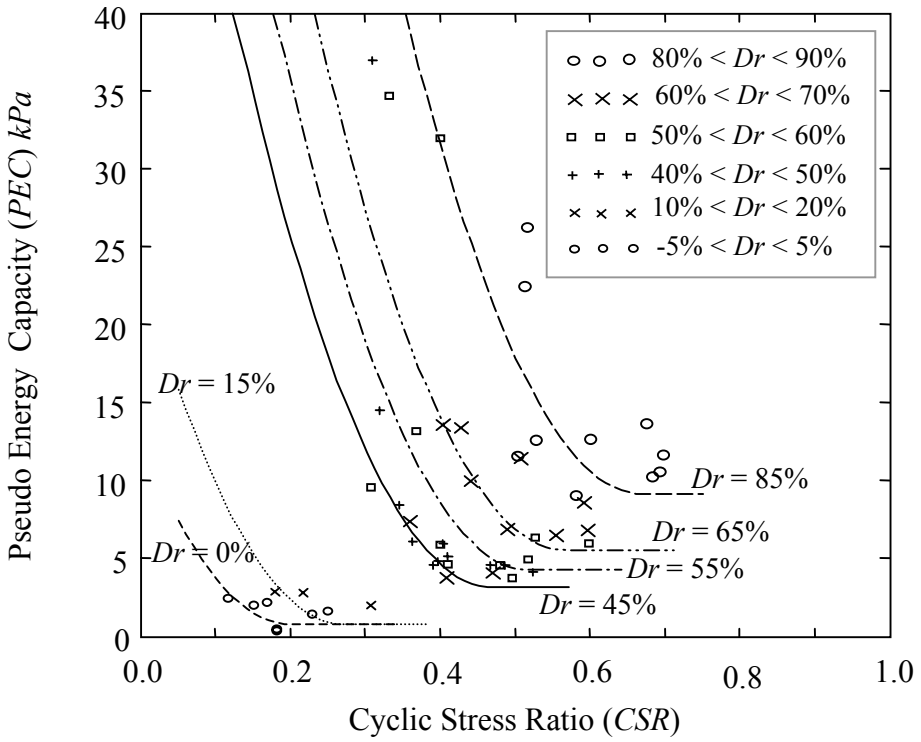

Figure 4-4. Correlations among *CSR*, *PEC*, and *Dr* for Monterey silt-sand mixtures ($FC \leq 30\%$).

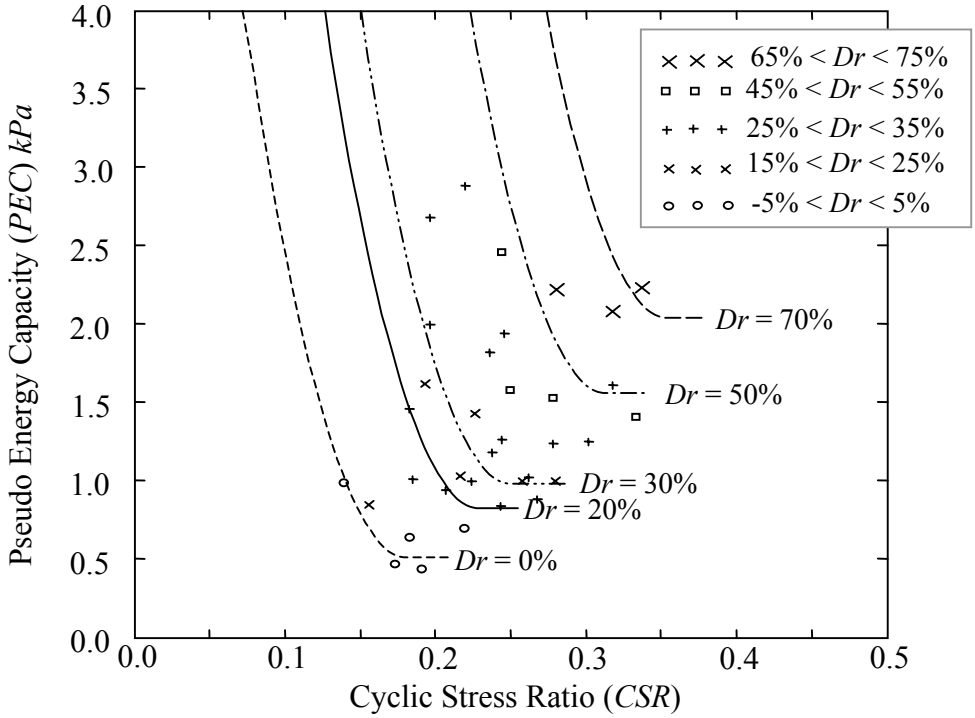

Figure 4-5. Correlations among *CSR*, *PEC*, and D_r for Yatesville silt-sand mixtures ($FC \leq 30\%$).

4.5 Load Dependency of Calibration Parameters

As stated in the introduction to this chapter, the dependence of the calibration parameters on the amplitude and frequency of the loading may limit the use of energy-based *Capacity* curves in the design of ground densification techniques. Conflicting conclusions are drawn from review of the published literature as to whether a unique relation exists between dissipated energy and pore pressure generation (i.e., if the calibration parameters are independent of factors other than the state variables of the soil, then a unique relation exists between dissipated energy and pore pressure generation).

Only two of the energy-based models presented in Section 4.2 provide correlations for their calibration parameters (i.e., *Hsu* and *FSKL* Models), and both expressions are functions of the amplitude of loading. Additionally, in presenting the results of a laboratory study conducted to validate the *DB1* Model, Simcock et al. (1983) state: "...it appears that pore pressure generation and dissipated energy are functionally related, but this relationship appears to depend strongly on the level of cyclic deviator stress." Because the soils, test apparatus, and control parameter for the loading (i.e., stress controlled versus strain controlled loading) differed among these studies, the load dependency of the calibration constants cannot be attributed to specific test conditions. On the contrary, Towhata and Ishihara (1985), Yanagisawa and Sugano (1994), and Wang et al. (1997) determined that the relationship between ΔW and r_u is independent of load path and amplitude of loading. The only commonality in these studies is the soil tested (i.e., Toyoura fine sand).

From examination of the correlations developed for the *GMP* Model's calibration parameter, given by Equations (4-16) and (4-17) and plotted in Figures 4-4 and 4-5, it can be seen that *PEC* increases rapidly below a certain *CSR*, which varies as a function of D_r. Alternate plots of the correlation for the Yatesville and Monterey silt-sand mixtures are shown in Figure 4-6a and 4-6b, respectively. Even though the same shape surface was used to fit the Monterey and Yatesville data, the dependency of *PEC* on *CSR* is more prominent in the medium grained Monterey sand than for the fined grained Yatesville

sand. There is no apparent reason for this dichotomy in the behavior of fine grained sands (e.g., Toyoura and Yatesville) and medium grained sands (e.g., Monterey).

The load dependence of *PEC* may be attributed to viscous drag. For a given frequency of applied loading (e.g., 1.0*hz*), the contribution of energy dissipated due to viscous drag increases as the amplitude of the applied loading decreases (Hall 1962). Of the three studies that showed load independency, Towhata and Ishihara (1985) used an extremely slow loading rate 0.14*% stain/min*, which would minimize the energy lost due to viscous drag regardless of the amplitude of the applied loading. Yanagisawa and Sugano (1994) used 1.0*hz*, and Wang et al. (1997) used a loading rate ranging from 0.01 to 1.0*hz* (Kuwano 2000). Additional laboratory data is required to resolve the load dependency issue.

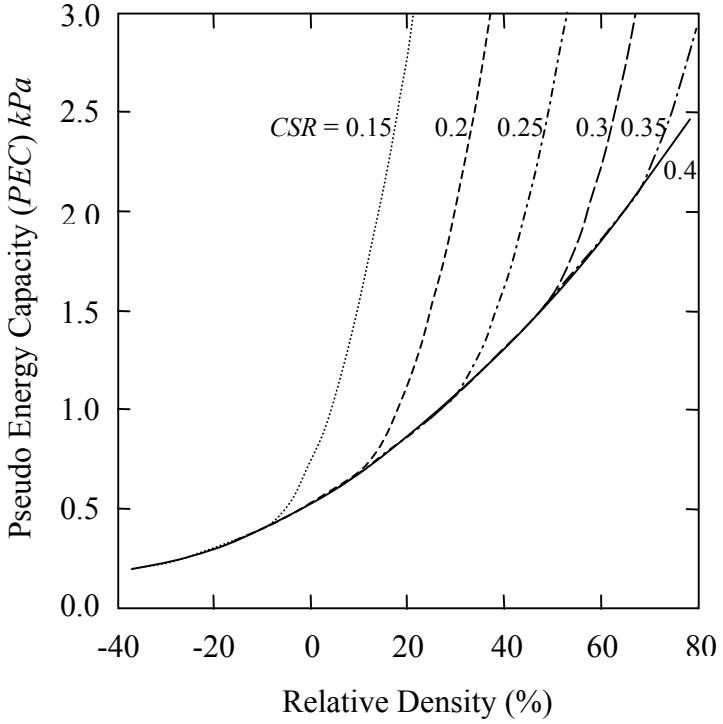

Figure 4-6a. Alternate plot of the correlation relating *PEC*, D_r, and *CSR* for Yatesville fine grained sand-silt mixtures.

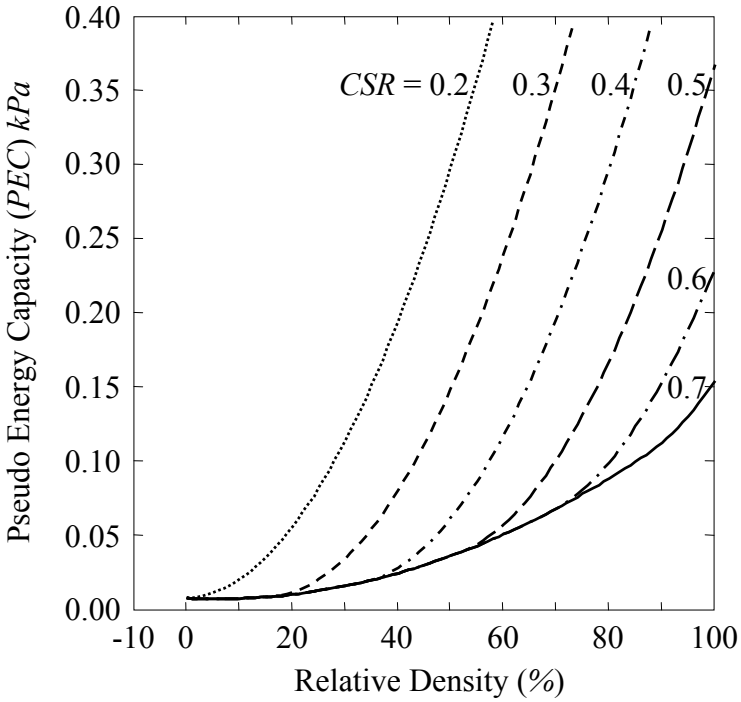

Figure 4-6b. Alternate plot of the correlation relating *PEC*, D_r, and *CSR* for Monterey medium grained sand-silt mixtures.

4.6 Summary

A review of published excess pore pressure generation models was presented. Particular emphasis was placed on examining the dependence (or independence) of the models' calibration parameters on factors other than the soil's state variables. The reason for this is that the dependence of the calibration parameters on such things as the amplitude of the loading, as well as state variables, may inherently limit the use of liquefaction curves developed from earthquake case histories for remedial ground densification design. Conflicting conclusions are drawn from the review of the literature and from the analyses of numerous cyclic tests. The only tentative conclusion is that the calibration parameters for fines sands appear to be less dependent on the amplitude and frequency of loading than for medium grained sands. Additional studies are required to determine why. In short, no conclusion can be drawn from the author's review excess pore pressure generation models as to the universality of dissipated energy for quantify the *Capacity* of cohesionless soil.